Heliyon 10 (2024) e26946

Contents lists available at ScienceDirect

Heliyon

journal homepage: www.cell.com/heliyon

Research article

Time-dependent biomechanical evaluation for corrective planning of scoliosis using finite element analysis – A comprehensive approach

Ahmad Alassaf [a], Ibrahim AlMohimeed [a], Mohammed Alghannam [a], Saddam Alotaibi [a], Khalid Alhussaini [b], Adham Aleid [b], Salem Alolayan [a], Mohamed Yacin Sikkandar [a,*], Maryam M. Alhashim [c], Sabarunisha Begum Sheik [d], Natteri M. Sudharsan [e]

[a] Department of Medical Equipment Technology, College of Applied Medical Sciences, Majmaah University, Al Majmaah 11952, Saudi Arabia
[b] Department of Biomedical Technology, College of Applied Medical Sciences, King Saud University, Riyadh 12372, Saudi Arabia
[c] Department of Radiology, College of Medicine, Imam Abdulrahman Bin Faisal University, Dammam, 34212, Saudi Arabia
[d] Department of Biotechnology, P.S.R. Engineering College, Sivakasi 626140, India
[e] Department of Mechanical Engineering, Rajalakshmi Engineering College, Chennai 602105, India

ARTICLE INFO

Keywords:
FEM
Transient analysis
Predictive simulation
Shape memory response

ABSTRACT

Scoliosis is a medical condition marked by an abnormal lateral curvature of the spine, typically forming a sideways "S" or "C" shape. Mechanically, it manifests as a three-dimensional deformation of the spine, potentially leading to diverse clinical issues such as pain, diminished lung capacity, and postural abnormalities. This research specifically concentrates on the Adolescent Idiopathic Scoliosis (AIS) population, as existing literature indicates a tendency for this type of scoliosis to deteriorate over time. The principal aim of this investigation is to pinpoint the biomechanical factors contributing to the progression of scoliosis by employing Finite Element Analysis (FEA) on computed tomography (CT) data collected from adolescent patients. By accurately modeling the spinal curvature and related deformities, the stresses and strains experienced by vertebral and intervertebral structures under diverse loading conditions can be simulated and quantified. The transient simulation incorporated damping and inertial terms, along with the static stiffness matrix, to enhance comprehension of the response. The findings of this study indicate a significant reduction in the Cobb angle, halving from its initial value, decreasing from 35° to 17°. In degenerative scoliosis, failure was predicted at 10^9 cycles, with the Polypropylene brace deforming by 10.34 mm, while the Nitinol brace exhibited significantly less deformation at 7.734 mm. This analysis contributes to a better understanding of the biomechanical mechanisms involved in scoliosis development and can assist in the formulation of more effective treatment strategies. The FEA simulation emerges as a valuable supplementary tool for exploring various hypothetical scenarios by applying diverse loads at different locations to enhance comprehension of the effectiveness of proposed interventions.

* Corresponding author.
E-mail address: m.sikkandar@mu.edu.sa (M.Y. Sikkandar).

https://doi.org/10.1016/j.heliyon.2024.e26946
Received 23 November 2023; Received in revised form 21 February 2024; Accepted 21 February 2024
Available online 28 February 2024

1. Introduction

Adolescent Idiopathic Scoliosis (AIS) is a common spinal deformity affecting approximately 2–3% of the adolescent population, with a higher prevalence among females [1,2]. It is characterized by a lateral curvature of the spine greater than 10°, along with vertebral rotation, and often affects the thoracic and lumbar regions of the spine [3–5]. The progression of AIS can lead to severe health problems, including pain, decreased pulmonary function, and reduced quality of life. While non-surgical treatments such as bracing can be effective in slowing the progression of the deformity, surgery is often necessary to correct the spinal curvature and prevent further progression of the deformity. The standard approach to surgical planning for AIS involves using radiographic imaging to assess the severity of the curvature and determine the appropriate surgical approach. However, radiographic imaging only provides a static view of the spine and does not account for the dynamic mechanical behavior of the spine. This can lead to suboptimal surgical outcomes and postoperative complications. Finite Element Analysis (FEA) is a computational method that allows for the simulation of the dynamic mechanical behavior of biological tissues and structures. In recent years, FEA has been increasingly used in the field of biomechanics for the evaluation of spinal deformities and surgical planning [6,7]. Time-dependent FEA allows for the simulation of the dynamic response of the spine to external loads and surgical instrumentation over time. The scientific question being investigated in this study is the application of time-dependent FEA for the evaluation of AIS and surgical planning. The study aims to develop a comprehensive methodology for using time-dependent FEA in evaluating AIS and surgical planning, including patient-specific modeling, boundary and loading conditions, FEA simulations, validation, and clinical application. By applying the possible loading conditions and constraints on different vertebrae on the digital twin, it would be possible for the surgeon to have a better understanding of the use of the right instrumentation at the right location. This would help in a better prognosis.

Mo and Cunningham (2011) summarized that the early detection of pediatric scoliosis by school nurses or doctors during routine spine examinations or changes in height is crucial. A diagnosis of scoliosis is made through spine radiographs with a coronal curvature measurement of at least 10°. Treatment options include serial observation, bracing until skeletal maturity, or surgery for severe or increasing deformity. The effectiveness of non-operative therapy is impacted by the cause of the deformity, careful follow-up, and patient compliance with the treatment regimen. Scoliosis should be intermittently monitored throughout adulthood to detect late deformity advancement, the onset of arthritic symptoms, or other related problems [8]. Wei et al. (2022) suggested that bracing is a commonly used conservative treatment for AIS [9]. Recently, there has been a growing interest in using FEA to improve the outcomes of brace therapy for AIS. Zhang et al. (2021) outlined a three-dimensional finite element model used to investigate the biomechanical changes of the lumbar spine segment of idiopathic scoliosis under different loads [10]. The model was based on the CT scan data of an AIS patient and included finely reconstructed tissue structures. The results showed that the range of motion is reduced under all loads in patients with AIS. The stress distribution was greater on the vertebral concave side under flexion loads, while under extension lateral bending and rotation loads, the stress was concentrated in the L3 vertebral arch. The intervertebral disc had the weakest buffering effect on rotational load, and the stress showed a trend of local concentration on the concave side of the scoliosis. The lumbar vertebrae comprising the greatest curvature experienced the most excessive stress, and the intervertebral disc was more likely to be injured under rotational load compared to other kinds of loads.

Cheng et al. (2010) addressed the impact of various loading situations on the differences in Cobb's angle and vertebral rotation in C-type scoliotic spines using FE modeling [12]. The right thoracic type (37.4°) with an apex above T7 was the geometry of the scoliotic FE model, which was built from C7 to L5. A medial-lateral (ML) and anteroposterior (AP) force with magnitudes of 100–0, 80–20, and 60-40 N were the three loading conditions considered. The AP force was dominant in changes to the axial vertebral rotation, whereas the ML force was dominant in changes to Cobb's angle. The level under the apex was the best level to use force to treat C-type scoliosis. Guan et al. (2020) determined the three-dimensional corrective force to reduce spinal deformity in AIS using FE analysis [13]. The vertebral structure is a primary load-carrying member of the human body and plays a critical role in its regular physical movements while standing, sitting, or walking. The repeated cycles of loading on the spinal segments give rise to the phenomenon of fatigue. Although studies have attempted to develop implants by considering fatigue [14], limited studies exist on the evaluation of fatigue life of the spinal structure [15,16].

In recent years, there has been a growing interest in the use of shape memory alloys, such as Nitinol, for the treatment of scoliosis. Nitinol is a unique material that can "remember" its shape and return to it after being deformed. This property makes it an ideal material for use in medical devices, including orthopedic implants and braces. The use of Nitinol braces for scoliosis treatment offers several advantages over traditional braces. Nitinol braces are more flexible, lightweight, and have a better shape memory than conventional braces, which can improve patient comfort and compliance. Additionally, Nitinol braces can exert a continuous and controlled corrective force on the spine, which can prevent the progression of the curvature and reduce the need for surgery [17–19]. Wang et al. (2011) conducted a retrospective study on the clinical and radiological outcomes of using a Nitinol shape memory alloy rod for the treatment of scoliosis [17]. It was found that using a Nitinol shape memory alloy rod intraoperatively was a safe and effective method for treating scoliosis. The use of Nitinol rods resulted in significant improvements in both clinical and radiological outcomes, with reduced complications and improved correction of the spinal curvature. The study demonstrated the potential of using Nitinol shape memory alloys in the treatment of scoliosis, providing a promising alternative to traditional treatment methods. Sánchez et al. (2012) induced structural experimental scoliosis in a rat model by tethering sutures between the left scapula and pelvis [18]. The scoliosis and resulting structural deformities of the vertebrae were then gradually corrected using a shape-memory alloy wire attached to the spine after the posterior tether was removed. It was predicted that by keeping constant corrective force loading on the still-growing spine, a straight shape-memory alloy wire implanted in the spine would offer better progressive repair of scoliosis and vertebral body defects. Wever et al. (2002) investigated based on the characteristics of the nickel-titanium alloy, a new scoliosis correction device's biocompatibility and functioning [19]. With the device, a gradual three-dimensional scoliosis correction is

accomplished using the shape recovery forces of a shape-memory metal rod. Notably, it was observed that before beginning clinical trials, the entire system should undergo extensive fatigue testing.

From the review of the literature, a few important observations are drawn. The vertebral stress response has been investigated under different static loads $\leq$100 N [12]. However, the time-dependent (transient) response of the human spine suffering from AIS remains to be investigated. Regarding the pathogenesis of scoliosis, the effect of static loads at different stages of progression has been studied [20]. However, the effects of cyclical loading on the fatigue life and stress assessment in AIS have not been scrutinized. As a corrective measure, the required force in braces for the effective improvement of AIS has been examined [13]. But importantly, the effectiveness and potential impact of the brace on the body has not been fully defined for reducing discomfort and improving patient outcomes. Also, shape memory alloy (SMA) braces need to be compared alongside the conventional materials. FEA can be a useful tool in exploring and evaluating these scenarios.

The primary objective of this study is to identify the biomechanical factors contributing to scoliosis progression by employing FEA on MRI data obtained from adolescent patients. By accurately modeling the spinal curvature and associated deformities, the stresses and strains experienced by the vertebral and intervertebral structures under different loading conditions can be simulated and quantified. Furthermore, this study aims to explore the influence of the duration of strain on the progression of scoliosis. By assessing the effects of sustained strain on the spinal structures over time, insights into the relationship between strain duration and scoliosis progression can be gained. This analysis can help elucidate the underlying biomechanical mechanisms involved in scoliosis development and aid in designing more effective treatment strategies. FEA simulations are thus used as valuable adjunct tools to study the various "what-if" scenarios by applying various loads at various locations to better understand the effectiveness of the proposed interventions for better prognosis.

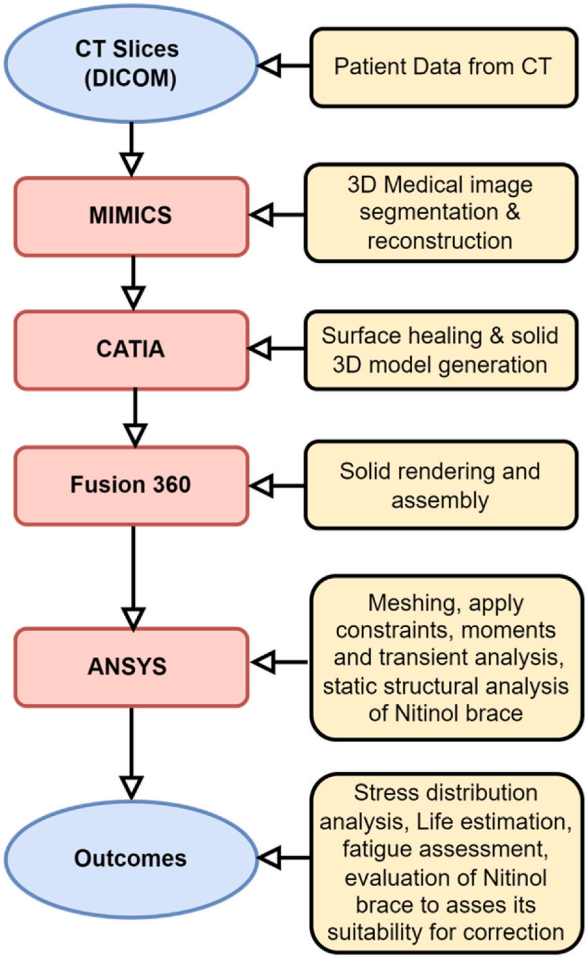

Fig. 1. Flowchart of the work.

2. Materials and methods

2.1. Dataset

50 CT images of Scoliosis digital images were collected from King Fahad Specialist Hospital, King Fahad Medical City (KFMC), Dammam, Saudi Arabia to carry out this research. The Institutional Review Board (IRB) of KFMC has reviewed and approved this study with research protocol (EXT0397) with IRB Log number 22-049E. Scoliosis at various regions of the spine in the age group (20 and 80 years including both Male and Female) were collected during the year 21 February 2022 to 20 February 2023 and the data were authorized to use for research purposes only. The Ethics committee waived the need for informed consent. Clinical experts clinically and manually classified these images. The Study started with an initial CT scan of a patient in DICOM format which consisted of image slices of the spine in axial, coronal, and sagittal orientations. The DICOM image file had a total number of 531 slices of 0.625 mm. Bone with dimensions 512 mm $\times$ 512 mm $\times$ 531 mm and spacing of 0.324 mm $\times$ 0.324 mm $\times$ 0.31 mm for volume rendering.

2.2. Methodology

As discussed in the literature, the reason for the progression of AIS for various subjects as well as the reason for the drying of the disc (desiccation) a cause of degenerative scoliosis is unknown. Simulation of the spine by varying the load conditions, type of loading (cyclic), as well as material property of the disk to mimic the drying of softer disk specific to each patient, can be done to understand the outcome due to various scenarios. Similarly, the non-surgical corrective action due to braces can also provide better insights. Thus, to understand the effectiveness of FEA for better intervention, the following analyses are performed on patient-specific CT image data about a scoliotic spine to obtain a three-dimensional geometrical model. Firstly, the length from C7 to L5 was modeled and loaded appropriately to understand the progression of AIS. Secondly, L1 to L5 alone was segregated and processed with the softer disks by subjecting them to cyclic loading to understand degenerative scoliosis and thirdly, the effect of braces under stress and conversely on the body is simulated. Ansys is used for the FEA simulation. The overall methodology of the proposed is depicted in Fig. 1.

The following three cases are considered for the FEA simulations:

i. Adolescent idiopathic scoliosis progression over time.
ii. Lumbar spine degenerative scoliosis at various loads.
iii. Analysis of the scoliotic spine by using shape memory material such as Nitinol braces to study its effectiveness in correcting the Cobb angle.

The patient-specific CT image of a scoliotic spine is processed to prepare the three-dimensional geometrical models for the first two analyses. For the third analysis, a brace is modeled using CAD software. Figs. 2 and 3 depict the segmentation process for the scoliotic spine model and scoliotic lumbar spine segment models respectively.

The post-processed model showed a clear and accurate representation of the spine, with minimal noise and artifacts as shown in Fig. 4(a) and (b), for the scoliotic spine and lumbar segment models, respectively.

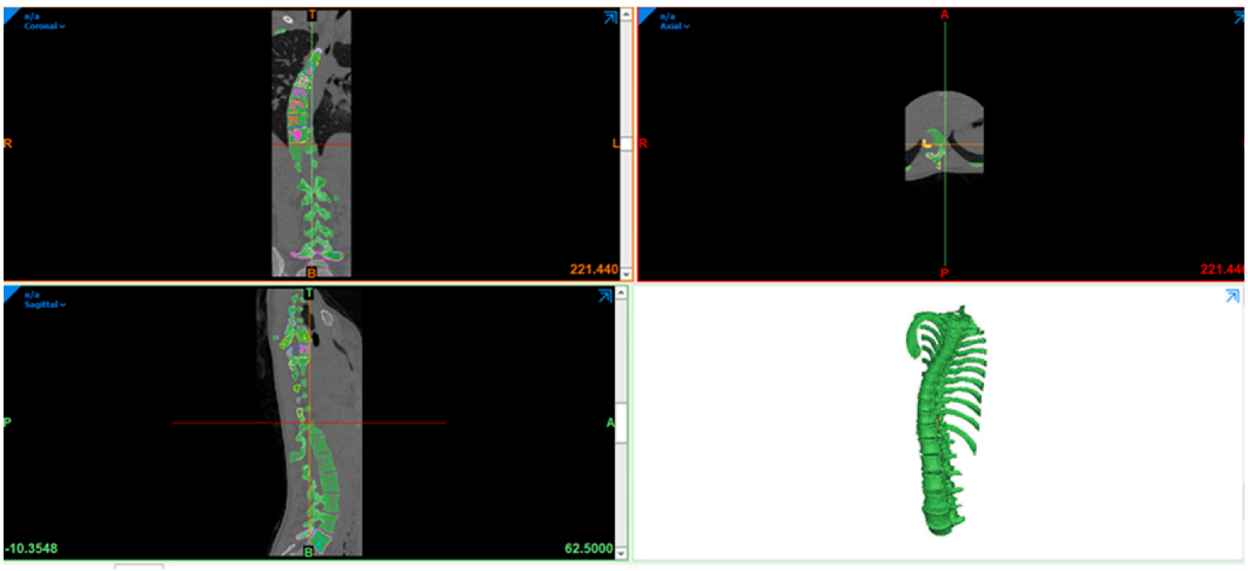

Fig. 2. Image segmentation process of the scoliotic spine.

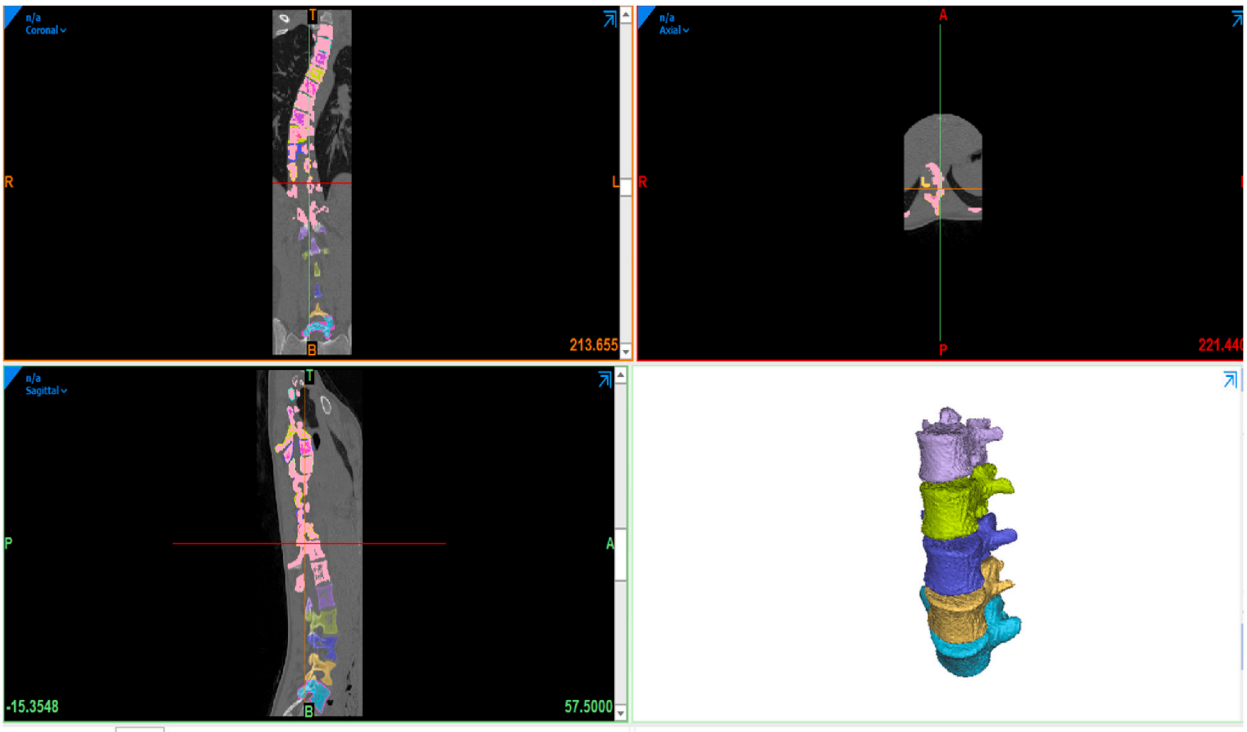

Fig. 3. Image segmentation process of the scoliotic lumbar spinal segment.

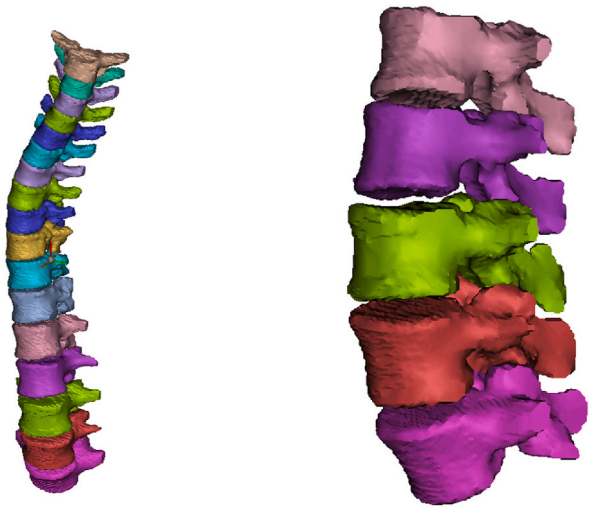

(**a**) (**b**)

Fig. 4. Post-processed models: (a) scoliotic whole spine; (b) scoliotic lumbar segment model.

2.3. Surface model (3D solid model) preparation

Figs. 5 and 6 depict the developed three-dimensional (3D) models for the entire spine and lumbar segment, along with the corresponding nomenclature. These 3D models are utilized for Finite Element Analysis (FEA) studies on transient and fatigue behavior in degenerative scoliosis patients. The solid models in Fig. 5a are then prepared for transient and fatigue analyses in ANSYS Workbench. Cobb angle analysis in Fig. 5b reveals a 35.4° angle for the untreated spine. Fig. 6 (a and b) represents the CAD model of AIS lumbar spine segment and its rendered view. Cobb angles exceeding 20–25° may necessitate interventions such as bracing or surgery. The FEA analysis predicts changes in Cobb angle under load, aiding clinicians in planning treatments based on transient analysis results.

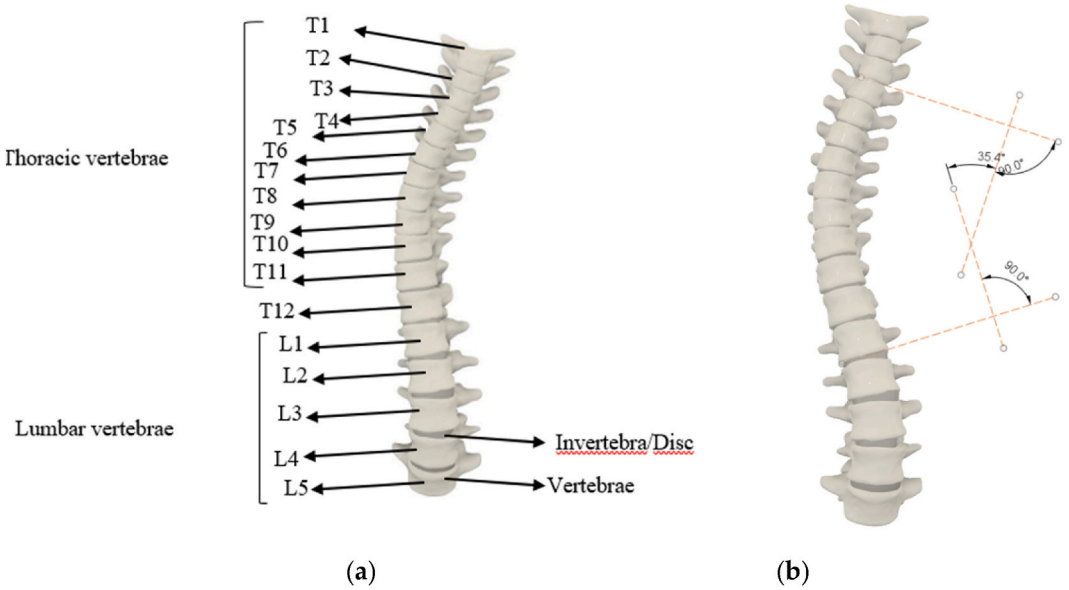

Fig. 5. (a) CAD model of AIS spine with nomenclature; (b) Cobb angle measurement.

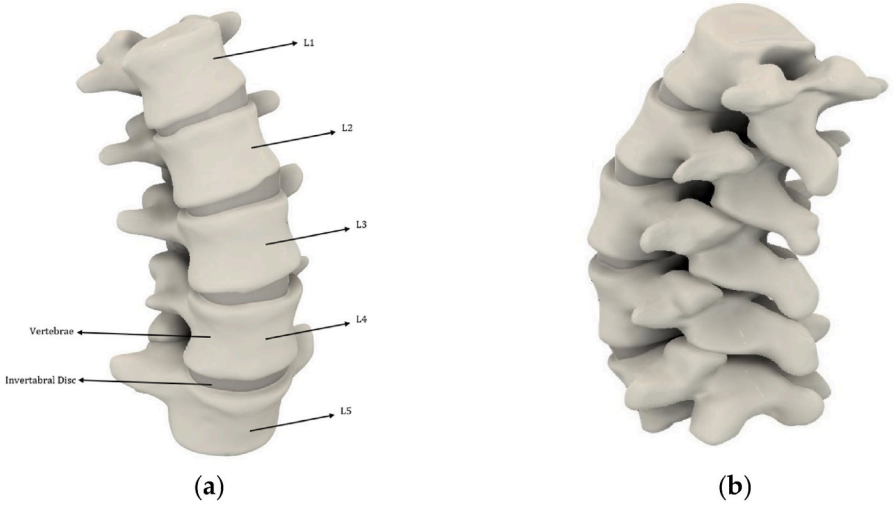

Fig. 6. (a) CAD model of AIS lumbar spine segment; (b) rendered view.

To create a 3D representation of a scoliosis brace, it was begun by acquiring precise measurements through a CT scanning process. These measurements are then imported into Fusion 360 software, where a series of specialized tools are utilized to craft a robust, comfortable, and seamless 3D model of the brace. This detailed model is subsequently fitted onto a human mannequin for evaluation and refinement. The accuracy of the initial measurements and the meticulous design process are crucial aspects of this procedure. Ensuring that the brace is both precisely contoured and comfortable for the wearer is of utmost importance. Ultimately, this meticulous process enhances the brace's effectiveness in addressing the condition it is designed for. In Fig. 7(a) and (b), we present the computer-aided design (CAD) model of the brace, highlighting its detailed structure and how it integrates seamlessly with the human body, demonstrating the meticulous work that has gone into its development.

2.4. Finite element modeling: meshing, material properties and boundary conditions

2.4.1. Time-dependent progression assessment of AIS

The geometric representation of Adolescent Idiopathic Scoliosis (AIS) is meticulously refined through a process called meshing, utilizing tetrahedral elements. Tetrahedral meshing stands out as a preferred method for modeling the spine in Finite Element Analysis (FEA) due to its array of advantages. This technique excels at capturing the intricate and irregular shapes of vertebrae and

(a) (b)

Fig. 7. (a) Brace CAD model; (b) Brace CAD model attached to the human body.

intervertebral discs, which are inherent complexities of the spine's structure. Furthermore, it is adept at providing highly accurate surface approximations, a crucial factor in ensuring precise calculations of stress and strain in biomechanical analyses. A detailed examination of the mesh was conducted through a mesh convergence study, leading to the development of a well-optimized mesh configuration. This refined mesh comprises a total of 150,634 nodes and 80,843 elements, attesting to the care taken to ensure the accuracy of the model. The culmination of this process is visible in Fig. 8a, which presents the converged meshed FEA model of the scoliotic spine, showcasing the painstaking detail and precision invested in the modeling process.

To establish the necessary boundary conditions for the simulation, all degrees of freedom were firmly constrained at the base of the spine. Additionally, a force of 300 N was applied, as illustrated in Fig. 8 (b), adhering to the methodology outlined in Refs. [10,21]. This is briefly described here. The loading and boundary conditions were based on available literature and briefly described here. Qiaolin Zhang [10] did a finite element analysis of L1 to L5 segments obtained from a CT of a 14-year-old girl who weighed 45 kg. The anteroposterior and lateral X-rays of the lumbar spine showed frontal Cobb and lumbar lordosis angles of 43° and 45°. The image was segmented using Mimics 20.0 and imported to solid works 2020 to form the solids. Ansys 19 was then used to simulate various loads. Based on the six loads studied invitro by Yamamoto et al., on three-dimensional movements of the whole lumbar spine and lumbosacral joint [11], 10 Nm moment was used and 300 N corresponding to 45 kg was applied as axial load. It was concluded that stress in intervertebral disk was higher in rotating loads and likely to get injured. Also, the range of motion gets affected and limited due to the shape of the vertebrae.

Rohlmann et al. [21] performed an FE analysis by incorporating an artificial disk. The L3 vertebra was subjected to pure moment of 7.5Nm in the three main anatomical planes to simulate flexion, extension, lateral bending to the right, and left axial torsion. The rotation and contact forces in the facet joints can vary depending on the implant radius, gap etc., And certain combination of loading may lead to higher forces that may be a cause for concern.

A free-body diagram of Fig. 8b is schematically represented in Fig. 8c for just two disks and the same is discussed in detail in Section 3.1. Table 1 offers a comprehensive compilation of the material properties applied throughout the FEA, providing valuable insights into the materials used and their corresponding properties [22–24]. The simulation was meticulously tracked over a 4-s duration, with measurements recorded at 1-s intervals. This comprehensive approach allows for a thorough exploration and analysis of the dynamic

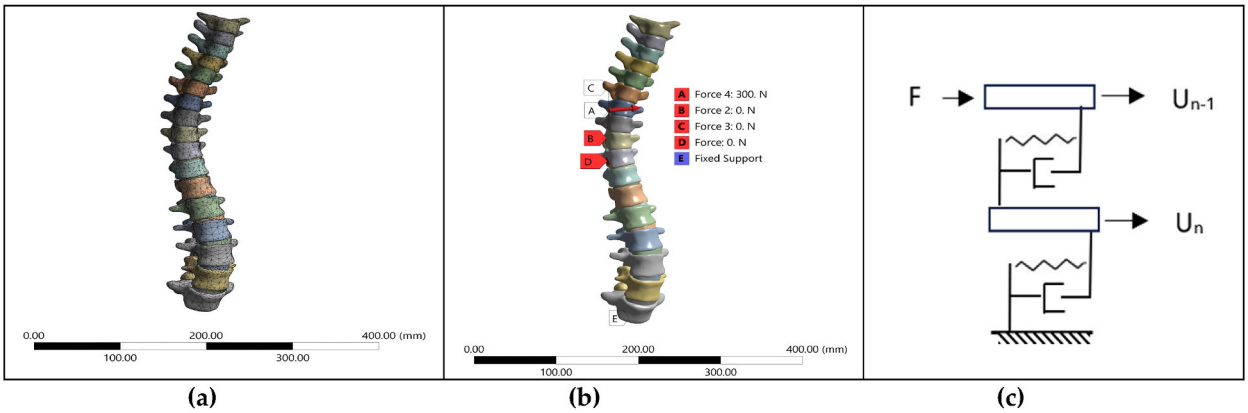

(a) (b) (c)

Fig. 8. (a) Meshed model of the scoliotic spine; (b) post application of boundary conditions and loads; (c) free body diagram.

Table 1
Material properties used in the transient-structural and fatigue analysis [22–24].

Description	Density (kg/m^3)	Youngs Modulus (MPa)	Poisons Ratio
Vertebrae	1850	1000	0.3
IVDs	1100	100	0.2

behavior of the spine, shedding light on its response to the applied forces and constraints.

2.4.2. Fatigue life and damage assessment of lumbar spine degenerative scoliosis

Because of the significant advantages that tetrahedral elements offer in efficiently representing intricate and complex geometries, particularly the vertebrae and intervertebral discs, they were chosen as the primary modeling tool for conducting fatigue analysis on the lumbar spine. To ensure the precision and reliability of the model, a thorough mesh convergence analysis was undertaken, leading to the selection of 50,522 nodes and 27,559 elements to construct the Finite Element (FE) model, as depicted in Fig. 9a. To create realistic conditions for the analysis, several boundary conditions and forces were applied. At the base of the lumbar segment, a fixed constraint was imposed, mimicking the anchoring effect of the pelvis. Furthermore, a vertical force of 700 N was applied, simulating the load experienced by the lumbar spine during flexion movements, as per reference [25]. Additionally, a lateral force of 10 N was introduced to replicate the forward-leaning motion of the body, without the influence of any external weight. This force helps to examine the structural response of the spine to such movements. In Fig. 9b, the graphical representation of these applied forces can be observed.

Moreover, to account for the rotational aspects of the spine's behavior, a moment of 10 N-m was applied. This moment serves to simulate the torque or rotational forces that the spine might experience during various activities and is displayed in Fig. 9b. The force moment pattern is shown in Fig. 9c. The values used here are comparable to those in open literature as was explained in the previous section. From the review it is seen that FE has its limitation as to provide for a value to decide on the onset of AIS. It is to be noted that FE can be a valuable adjunct tool for the surgeon to understand the propagation of stresses and deformation of the spine to decide on the method of intervention. Hence no specific threshold can be suggested.

By incorporating these boundary conditions and forces, the analysis aims to provide a comprehensive understanding of how the lumbar spine responds to both external loads and internal biomechanical interactions, shedding light on its behavior during activities involving flexion, lateral motion, and rotation.

Fatigue analysis was conducted employing Soderberg's method, involving 10^9 cycles of loading, with the primary objective of establishing the endurance limit of materials when subjected to repeated and cyclic stresses. This analysis also delved into the evaluation of the lifespan of the lumbar spine, the extent of damage sustained during the cyclic loading, and the associated safety factors. As a possible method of approach this protocol to the spine that had already deformed due to Scoliosis. The application of cyclic loading, crucial for understanding how the lumbar spine withstands repetitive stresses, is visually depicted in Fig. 10. Here the first image of the ordinate depicts the constant amplitude loads in both directions. This is a representation and does not have any specific unit. In the abscissa, the cycles are shown. Here again, this is based on the empirical S–N curve and corrected using Soderberg mean stress correction. These are built in models in ANSYS, and detailed explanations are out of the scope of the present work. The readers may refer to the various fatigue analysis models available in open literature. A typical correction based on Goodman. Soderberg and Gerberg are presented in the second image of Fig. 10. Soderberg's theory is overly conservative and is used for brittle materials whereas Goodman can be used for both ductile and brittle. The present work used Soderberg to be conservative. This analysis enables us to gain insights into the spine's capacity to endure cyclic loading, its susceptibility to fatigue-induced damage, and the safety margins in place to prevent structural failure.

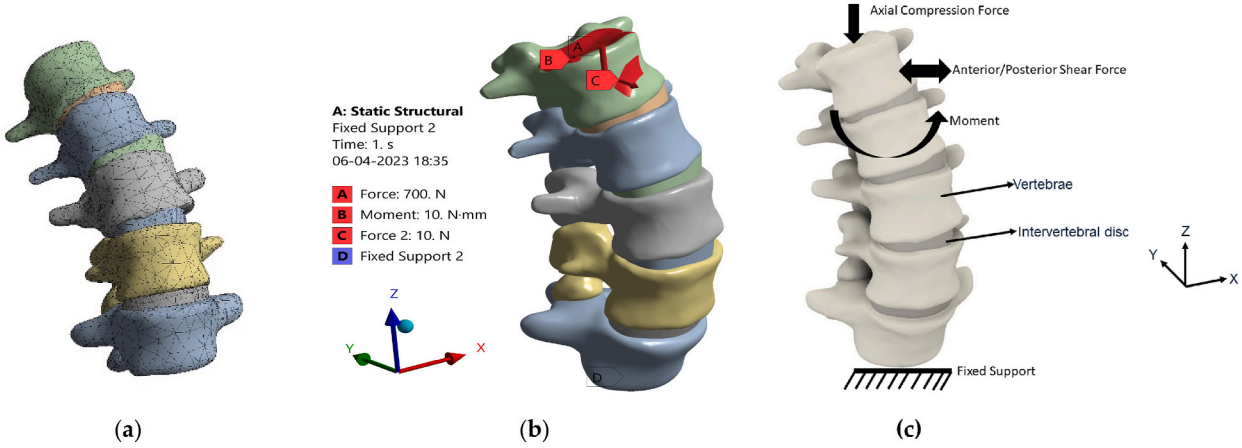

Fig. 9. (a) Meshed lumbar segment; (b) post application of boundary conditions and loads; (c) forces and moments pattern.

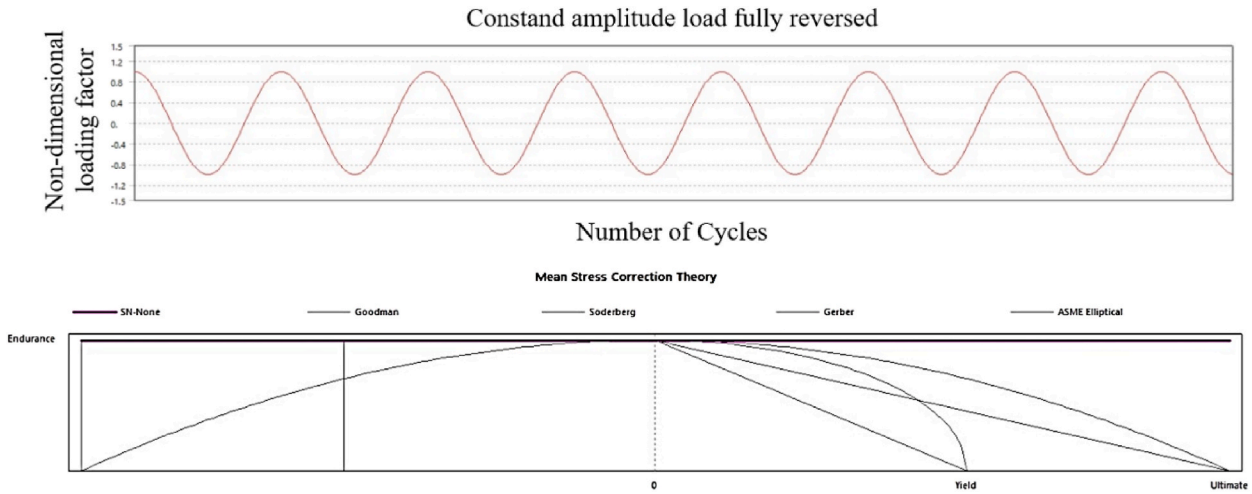

Fig. 10. Schematic representation of loading conditions set for fatigue analysis involving cyclic stresses.

2.4.3. Performance assessment of Nitinol scoliosis brace

Tetrahedral elements were utilized to represent the brace and the human body. In this case, the mesh converged with a total of 162,074 nodes and 86,329 elements (refer to Fig. 11a). To simulate the application of scoliosis corrective force by the brace on the human body, a lateral force of 300 N was applied (Fig. 11b) on each side of the brace, and the human body model is fixed at its base [10]. Table 2 shows the list of material properties considered during the analysis. Two brace materials, viz., Polypropylene and Nitinol, are considered in the present study. A static structural FE analysis is conducted to evaluate the performance and comfort of the two brace materials for the patients. The material properties for Nitinol were obtained from Ref. [26] and for other biomaterial implants from Ref. [27].

3. Results

3.1. Transient response of scoliotic spine

A free body diagram of Fig. 8b is schematically represented in Fig. 8c for just two disks. Here just two degrees of freedom of the disk is modeled with a massless spring and damper are shown. The joints are comprised of intervertebral disks and soft tissues. The spring element of each flexible joint structure obeys Hooke's law and is said to have a linear relationship F = kU where k is the stiffness of the

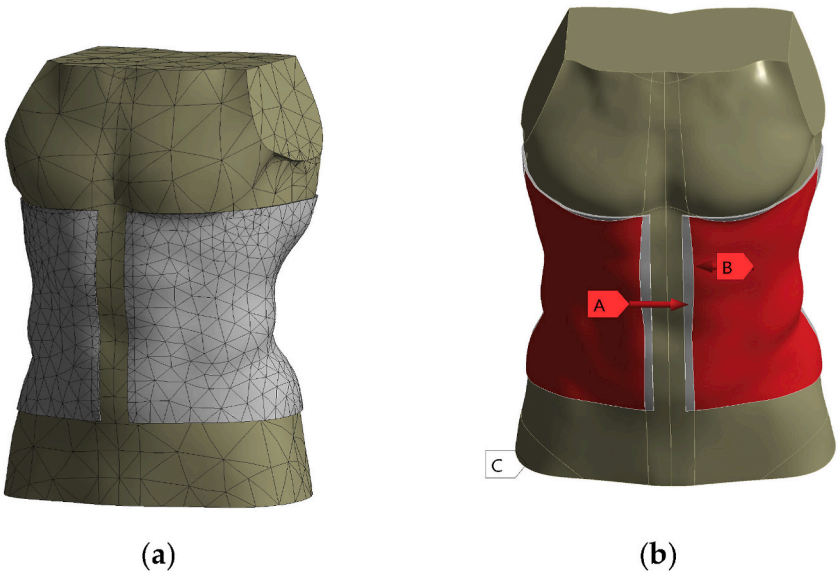

Fig. 11. (a) Meshed model for brace simulation; (b) post application of boundary conditions and loads (A – force 300 N, B – force 300 N and C – fixed support).

Table 2
Material properties used in the brace corrective force FE analysis.

Description	Density (kg/m^3)	Youngs Modulus (MPa)	Poisons Ratio
Polypropylene	900	1325	0.45
Nitinol	6450	35,877	0.33
Muscle (relaxed)	1084	39	0.47

spring and U is the deflection. The damper is assumed to behave as a Newtonian viscous fluid, F = c dU/dt where c is the damping coefficient (Ns/m). This system needs to account for the, (a) inertial forces, (b) dissipation forces, (c) restoring forces, and finally the external forces and is represented in Equation (1).

$$[K]\{U\} + [C]\{\mathring{U}\} + [M]\{\ddot{U}\} = \{F\}, \quad (1)$$

In this context, the initial term on the left side addresses displacement, while the subsequent two terms consider damping and inertial aspects. This equation is set equal to the externally applied force. When the simulation is conducted under static conditions, the influence of damping and inertial behavior is overlooked. Given that we are working with soft tissues designed to absorb shocks, it becomes crucial to undertake 3D transient modeling. As mentioned previously, the simulation has not accounted for the impact of load under transient conditions, and the current study focuses on tracking relevant parameters over time. Table 3 presents the deformation over time. The application of transient loads resulted in a maximum deformation of 0.3593 mm, which indicates the extent of flexibility in the spine under loading conditions. The maximum stress induced was 20.965 MPa, which represents the maximum force experienced by the spine. The maximum strain induced was 2.35E−02 mm/mm, which indicates the amount of deformation experienced by the spine relative to its original size. These values provide important insights into the biomechanical behavior of the spine under loading conditions and can be used to predict the effectiveness of different treatment options. A closer examination of the deformation induced due to load is maximum at the point where the load was applied (Fig. 12a). One can observe that the entire region the stress and the corresponding strain (Fig. 12b and c), are at the lower end of the spectrum (almost blue) and just one point has the maximum value. This point is where the load was applied. It is to be appreciated that there is no "point load" that has "zero area". This application of point load results in higher stress-strain values and that single value may safely be ignored. The maximum stress can be seen to be around 7 MPa and negligible strain.

The study revealed a noteworthy reduction in the Cobb angle, which decreased by half from its initial value, shifting from 35° to 17°, as visually represented in Fig. 13 (a and b). Additionally, the investigation delved into the distribution of stress and strain across each vertebra and intervertebral disc. Initially, the thoracic region exhibited a more pronounced curvature, but this curvature was notably mitigated following the analysis. This observation underscores the critical significance of tailoring treatment plans to accommodate the distinct characteristics of each patient's spinal curvature. It emphasizes the need to consider the individual nuances of a patient's condition to optimize the effectiveness of treatment strategies, thereby attaining better outcomes.

3.2. Fatigue life and damage assessment of scoliotic lumbar spine segment

Following a comprehensive examination of how transient loads impact the spine, the study turns its attention to understanding the potential consequences of fatigue and the resultant degeneration in the L1 to L5 region of the spine. The data collected after subjecting this region to fatigue loading is summarized in Table 4. This analysis allows us to gain insights into the long-term effects and potential wear and tear that may occur in the lumbar spine, specifically in the L1 to L5 region. The numerical values presented in Table 4 serve as critical indicators of the spine's response to sustained loading and the associated changes over time.

Upon a closer examination of the data presented in Table 4 and Fig. 14 (a, b and c), it becomes apparent that the observed

Table 3
AIS deformation, stress, and strain over time.

Deformation [mm]			
Time [s]	Minimum	Maximum	Average
1	0	0.28652	0.12795
2	0	0.26977	0.12549
3	0	0.30582	0.12499
4	0	0.3593	0.1243
Equivalent Strain [mm/mm]			
1	6.31E−11	8.45E−03	2.20E−04
2	6.10E−11	9.69E−03	2.14E−04
3	1.24E−10	1.54E−02	2.21E−04
4	1.10E−10	2.35E−02	2.42E−04
Equivalent Stress [MPa]			
1	5.56E−07	22.845	0.54547
2	3.53E−07	13.421	0.53745
3	1.21E−06	16.402	0.51991
4	1.10E−06	20.965	0.53784

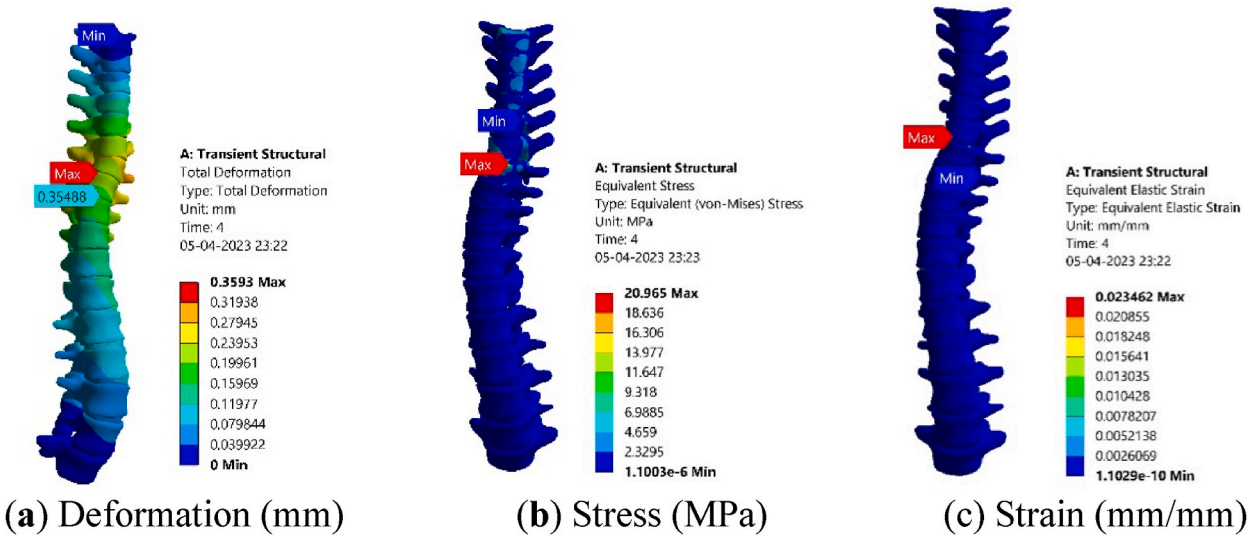

Fig. 12. Results of transient FE analysis.

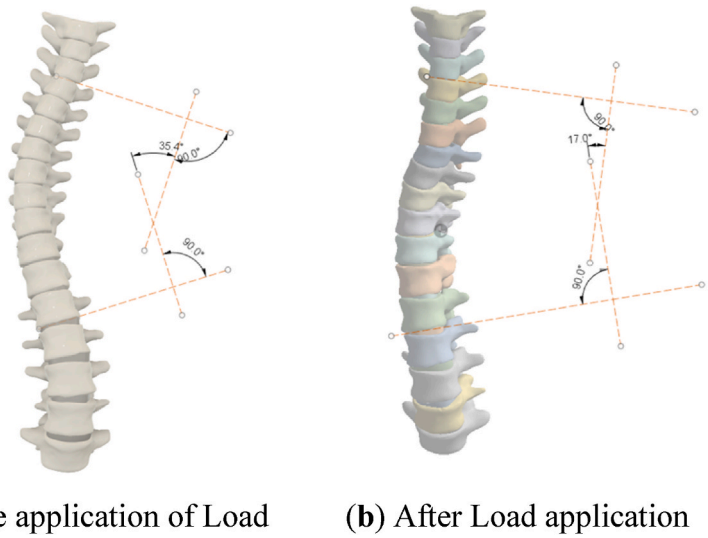

Fig. 13. Cobb angle before and after application of load in the transient FE analysis.

Table 4
Deformation, stress, and strain response to fatigue loading in the respective region of the spine.

Region	Deformation			Equivalent Stress			Equivalent strain		
	Minimum [mm]	Maximum [mm]	Average [mm]	Minimum [MPa]	Maximum [MPa]	Average [MPa]	Minimum [mm/mm]	Maximum [mm/mm]	Average [mm/mm]
All Lumber Spines	0	0.23951	9.73E−02	1.60E−05	15.204	0.89552	1.83E−09	2.02E−03	9.94E−05
L1	0	4.56E−02	2.42E−02	9.28E−05	12.019	0.80811	1.57E−08	2.02E−03	9.23E−05
L2	2.07E−02	7.85E−02	5.41E−02	5.67E−05	10.029	0.88229	6.08E−09	1.41E−03	9.80E−05
L3	6.21E−02	0.12209	9.08E−02	4.06E−05	7.7541	0.75216	4.74E−09	7.79E−04	8.45E−05
L4	8.99E−02	0.17586	0.13997	1.60E−05	15.204	0.6494	1.83E−09	1.62E−03	7.34E−05
L5	0.13599	0.23951	0.19478	4.04E−05	7.222	0.44106	4.25E−09	7.47E−04	4.89E−05

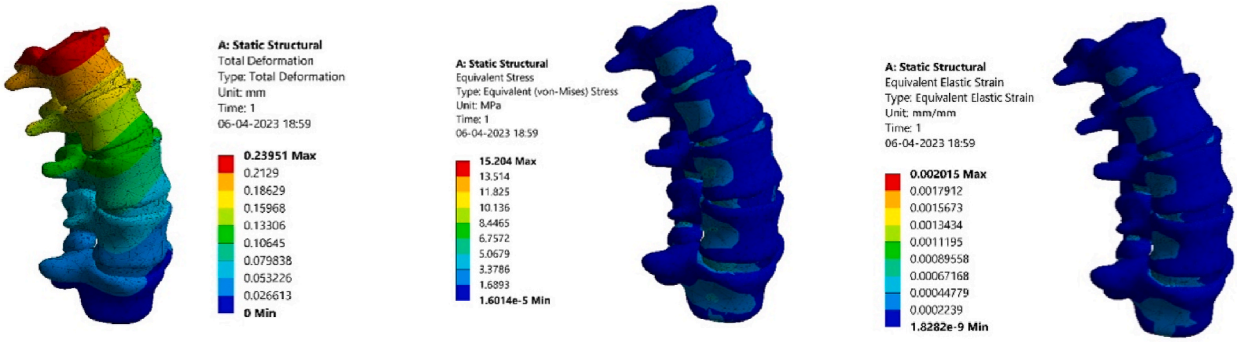

Fig. 14. Static-structural FE analysis results of the scoliotic lumbar spine.

deformations and the corresponding stress-strain values are notably minimal. However, the significance of these findings becomes clearer when we delve into the analysis of the effects induced by subjecting the material to a staggering one billion (10^9) loading cycles, as elaborated in Fig. 15 (a, b and c). The outcome of this extensive cyclic loading analysis in Fig. 15 sheds light on the stress-life relationship, the extent of accumulated damage, and the associated safety factors. Notably, it becomes evident that the system has reached a point of failure under these conditions. To gain a deeper understanding of the system's durability and limitations, it is possible to explore the impact of reducing the cyclic loading magnitude and the number of cycles. This approach allows for an estimation of damage accumulation and the corresponding safety margin. Such analysis is valuable in determining the system's tolerance levels and provides essential insights for devising intervention strategies. In essence, it helps in quantifying the point at which the system may surpass its capacity, enabling proactive measures to prevent failures and ensure its continued functionality.

3.3. Comparison of Nitinol brace with that of conventional materials

The simulation is conducted in two scenarios: one with just the brace, and the other with the brace encompassing the body. The outcomes, in terms of overall deformation, are documented in Table 5 for both scenarios. To provide a more detailed visual representation, Fig. 16 (a, b and c), Fig. 17 (a, b and c), Fig. 18 (a, b and c) and Fig. 19 (a, b and c) illustrate the distribution of deformation, stress, and strain. These figures showcase the behavior of both Polypropylene and Nitinol when attached to the body, as well as in isolation, offering a comprehensive view of how the materials interact with the body and influence the overall system. This analysis helps in understanding how the brace, when interacting with the human body, affects deformation, stress, and strain, which are crucial aspects in evaluating its performance and comfort for patients.

The results clearly indicate the notable differences in the behavior of the two types of braces. When subjected to an applied force, the deformation in the Polypropylene brace measured 10.34 mm, whereas the Nitinol brace exhibited significantly less deformation at 7.734 mm. This disparity underscores the superior ability of the Nitinol brace to maintain specific body positions effectively. The stress values further emphasize the distinctive characteristics of these materials. The Polypropylene brace exhibited a stress value of 4.738 MPa, while the Nitinol brace displayed a notably higher stress value of 26.628 MPa. This stark contrast highlights the remarkable shape memory behavior of Nitinol, enabling it to withstand external forces with greater resilience. The reduced deformation in the Nitinol brace is attributed to its unique property as a shape memory alloy. Nitinol undergoes a reversible phase transition between austenite and martensite phases. When deformed at a certain temperature, Nitinol stores the deformation in its martensitic state. Upon heating, it returns to the austenitic state, recovering its original shape. The phase transition allows Nitinol to endure significant strains without permanent deformation, making it suitable for applications where shape recovery is critical, such as medical devices and actuators. This characteristic allows it to be molded to conform to the patient's body shape when heated and then return to its original shape when cooled. Consequently, the Nitinol brace can provide more effective treatment by closely adapting to the patient's body shape, enhancing comfort and support.

Furthermore, the higher stress resistance exhibited by the Nitinol brace is directly linked to its shape memory behavior, which enables it to maintain its shape and withstand deformation even under significant stress. In summary, the advantages of the Nitinol brace over the Polypropylene brace encompass its enhanced ability to maintain specific body positions, superior conformity to the patient's body shape, and its capacity to withstand external forces more effectively. These qualities make the Nitinol brace a preferable treatment option for scoliosis, particularly for patients with severe curves or those requiring customized support. However, it's important to note that Nitinol braces may come at a higher cost, potentially limiting accessibility for some patients. Additionally, further research is necessary to comprehensively assess their long-term effectiveness and durability.

4. Discussion

In this study, the time-dependent mechanical responses of the scoliotic spine were investigated through a transient structural FE

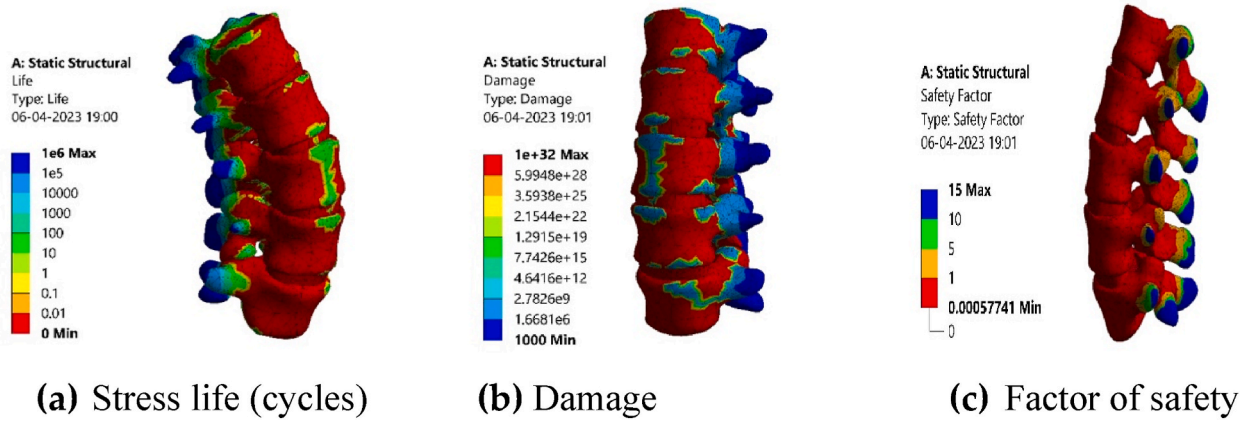

Fig. 15. Fatigue FE analysis results of scoliotic lumbar spine.

simulation. The results have indicated that an appropriate loading can induce a significant (around 50%) correction in the Cobb angle. Zetterberg et al. [28] measured the time-dependent changes in the Cobb angle in patients with adolescent idiopathic scoliosis under the action of self-weight (gravity), during approximately 12-h time periods. It was observed that, under the action of gravity, the upright standing and sitting position during the daytime further aggravates scoliosis, whereas the supine position (lying down on the back with the abdomen facing upwards) during the sleeping hours resulted in a correction in the Cobb angle of around 19 in the thoracic curve and 31% in the lumbar curve. Torell et al. [29] found that the supine position induces a mean scoliosis correction of around 9% through an analysis of 287 girls with idiopathic scoliosis. The present analysis considered a similar transversely directed loading scenario which showed a positive influence in correcting the scoliosis angle when sustained over a period. It needs to be kept in mind, however, that owing to the viscoelastic material components which make up the human spine, the deformations would happen in a much more gradual manner. Also, this kind of correction would be more appropriate in younger patients with a more flexible and immature skeletal system, which would more easily deform under the action of external loading [28].

Zhang et al. [30] investigated the response of scoliosis under orthotic treatment in the form of braces for patients suffering from moderate AIS. It was observed reduction in Cobb angle can be achieved after donning the braces. Recently, FE analysis has been used by other researchers as a predictor of the brace effect on scoliosis [31]. In the current analysis, it is revealed that Nitinol is superior to polypropylene braces for proper restraining force on the human body thereby providing better support to correct scoliosis. Therefore, the study quantitatively highlights the positive impact of Nitinol braces for scoliosis treatment. Spine deformities can be rectified or delayed by appropriate corrective strategies. Surgery or the use of braces are the options available. In surgery fusion of a few disks with the insertion of rods is done as a corrective measure. Each case is unique and requires experienced clinicians to assess the region of interest before embarking on the surgery. Knowing the exact number of bones to be fused and instrumentation can be now assessed non-invasively by performing numerical simulations and several 'what-if' analyses. The biggest advantage of FEA is that it can simulate various stress conditions a-priori to enable the surgeon to have a deeper understanding of the behavior of the spine to external stimuli. The authors hope that this will ensure a better prognosis and less need for repeat surgery. Where possible the brace would suffice, thereby relieving the patients from painful surgery. In the present work, the FEA simulation was performed under transient conditions to showcase the possible advantages of FEA as an adjunct tool. The patient calls are also taken into confidence as it becomes easier to demonstrate what the intervention and outcome would be. 3-D visualization would help a patient make an informed decision. Future work can include fusing the disks at the choice of the surgeon and visualizing the various outcomes. The ability to withstand fatigue loading without degeneration and effective tightening of braces with minimum discomfort are all possible before making the right intervention.

5. Conclusions

The FEA conducted in this study played a pivotal role in unraveling multiple facets related to Adolescent Idiopathic Scoliosis (AIS), encompassing the repercussions of degeneration under cyclic stress and the efficacy of employing two distinct materials – polypropylene and shape memory material – within a brace. A crucial insight gleaned from this analysis underscores the significance of integrating time-dependent factors, such as damping and inertial terms, into the structural equations. This integration proves indispensable for acquiring a comprehensive understanding of how the spine responds to stress over an extended duration. Of particular note, the study disclosed that the L1 to L5 region of the spine exhibited resilience under static loading conditions but manifested vulnerability and susceptibility to failure when subjected to cyclic loading. This observation underscores the imperative need to assess the spine's fatigue resistance on an individualized basis, considering the unique characteristics of each vertebra. Moreover, the research underscored the substantial role of braces as a non-surgical intervention in forestalling spinal deterioration. It accentuated the critical nature of judicious material selection and the implementation of appropriate pre-stressing techniques in brace design. These considerations are paramount for ensuring optimal comfort and support for the patient.

Table 5
Deformation, stress, and strain response to brace.

Material	Region	Deformation [mm]			Equivalent Stress [MPa]			Equivalent strain [mm/mm]		
		Minimum	Maximum	Average	Minimum	Maximum	Average	Minimum	Maximum	Average
Poly Propylene	Total	0	10.304	4.48E−01	0.00E+00	4.738	4.26E−02	0.00E+00	5.61E−01	7.65E−04
	Human Body	0	1.03E+01	5.13E+00	2.55E−05	2.15E−02	1.30E−03	9.46E−04	5.61E−01	3.77E−02
	Brace	7.36E−01	1.02E+01	6.93E+00	3.14E−02	4.738	0.84211	4.98E−05	3.83E−03	9.52E−04
Nitinol	Total	0.00E+00	7.7347	2.61E−01	0.00E+00	26.628	0.20614	0.00E+00	3.37E−01	4.42E−04
	Human Body	0.00E+00	7.7347	3.5446	2.12E−05	1.26E−02	7.72E−04	6.72E−04	3.37E−01	2.28E−02
	Brace	1.1499	7.0654	3.8262	5.66E−02	26.628	4.0727	2.36E−06	8.01E−04	1.78E−04

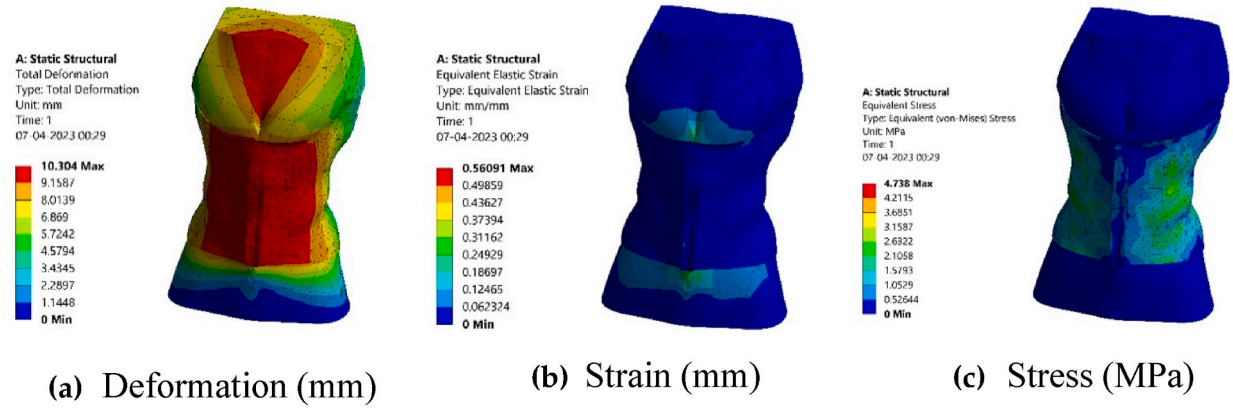

Fig. 16. Static-structural FEA results for body attached with polypropylene brace.

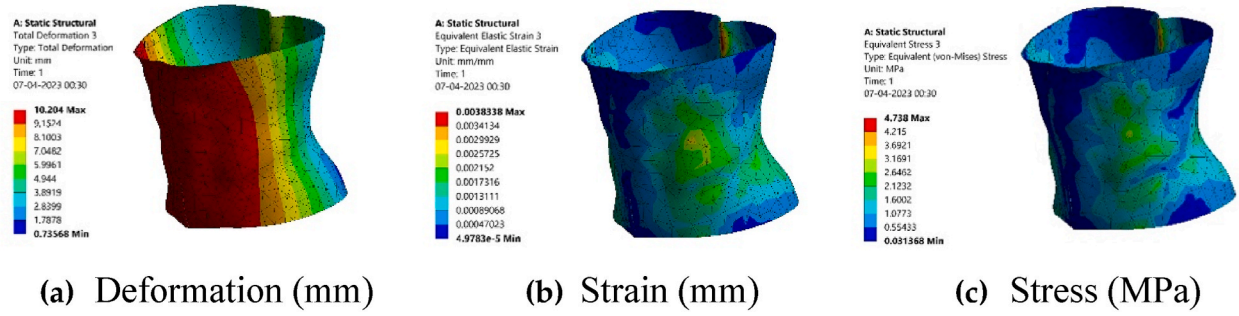

Fig. 17. Static-structural FEA results for the polypropylene brace.

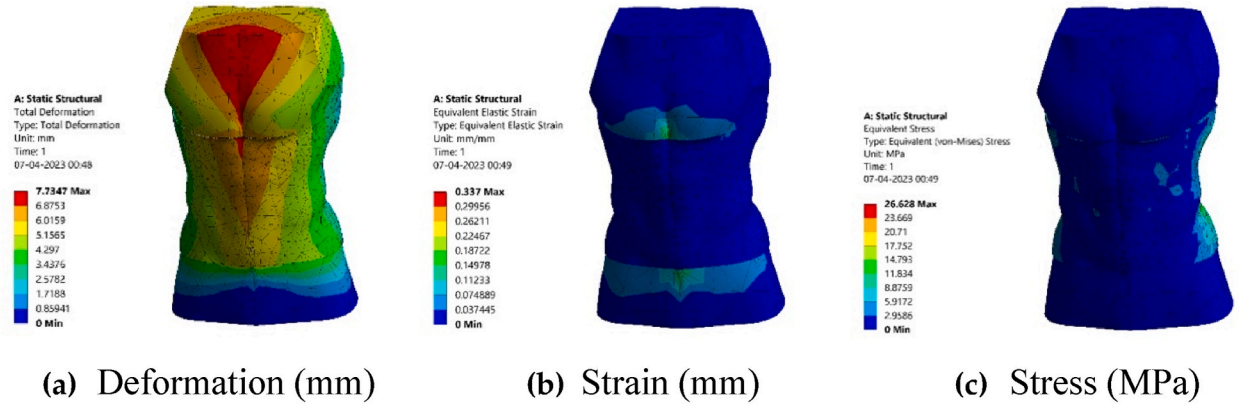

Fig. 18. Static-structural FEA results for body attached with Nitinol brace.

In summary, FEA simulations emerge as an invaluable supplementary tool for probing diverse hypothetical scenarios through the application of varying loads at distinct locations. This approach significantly contributes to enhancing our comprehension of the effectiveness of proposed interventions and strategies aimed at addressing scoliosis. It serves as a potent instrument for evaluating "what-if" scenarios and their potential impact on the spine, empowering healthcare professionals to make well-informed decisions regarding patient care and treatment strategies.

Funding

This research was funded by the King Salman Center for Disability Research for funding this work through Research Group Number

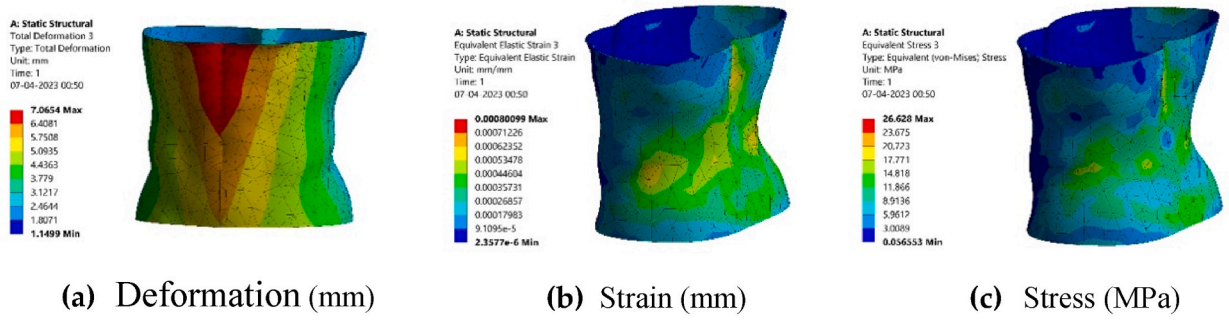

Fig. 19. Static-structural FEA results for the Nitinol brace.

KSRG-2023-339.

Institutional review board statement

The study was conducted in accordance with the Institutional Review Board (IRB) of Research Center, King Khalid Medical City (RC-KKMC), King Fahad Specialist Hospital Dammam (KFSHD) has reviewed and approved this study and research protocol (protocol code EXT0397 and 21 February 2022) with IRB Log number 22-049E.

Informed consent statement

Ethics committee waived the need for informed consent. Authors do not have access to information that could identify individual participants during or after data collection.

Data availability statement

Data availability in public domain is restricted due to privacy or ethical restrictions. Researchers needing access to this dataset may contact the corresponding author.

CRediT authorship contribution statement

Ahmad Alassaf: Data curation, Conceptualization. **Ibrahim AlMohimeed:** Resources, Formal analysis, Data curation. **Mohammed Alghannam:** Writing – original draft, Investigation, Formal analysis. **Saddam Alotaibi:** Writing – original draft, Formal analysis, Data curation. **Khalid Alhussaini:** Investigation, Formal analysis, Data curation. **Adham Aleid:** Methodology, Investigation, Funding acquisition. **Salem Alolayan:** Methodology, Investigation. **Mohamed Yacin Sikkandar:** Writing – original draft, Funding acquisition. **Maryam M. Alhashim:** Visualization, Validation, Resources. **Sabarunisha Begum Sheik:** Writing – review & editing, Software. **Natteri M. Sudharsan:** Writing – review & editing, Supervision.

Declaration of competing interest

Mohamed Yacin Sikkandar reports financial support was provided by King Salman Center for Disability Research for funding this work through Research Group Number KSRG-2023-339. If there are other authors, they declare that they have no known competing financial interests or personal relationships that could have appeared to influence the work reported in this paper.

Acknowledgments

The authors extend their appreciation to the King Salman Center for Disability Research for funding this work through Research Group Number KSRG-2023-339.

References

[1] D.M. Sproule, Scoliosis, in: Michael J. Aminoff, Robert B. Daroff (Eds.), Encyclopedia of the Neurological Sciences, second ed., Academic Press, 2014, pp. 112–114, https://doi.org/10.1016/B978-0-12-385157-4.00643-6. ISBN 9780123851581.

[2] Patrick D. Barnes, Chapter 9 - spine imaging, in: Johan G. Blickman, Bruce R. Parker, Patrick D. Barnes (Eds.), Pediatric Radiology, third ed., Mosby, 2009, pp. 271–296, https://doi.org/10.1016/B978-0-323-03125-7.00009-8. ISBN 9780323031257.

[3] Durga R. Sure, Michael LaBagnara, Justin S. Smith, Christopher I. Shaffrey, 158 - pediatric spinal deformities and deformity correction, in: Michael P. Steinmetz, Edward C. Benzel (Eds.), Benzel's Spine Surgery, 2-Volume Set, fourth ed., Elsevier, 2017 https://doi.org/10.1016/B978-0-323-40030-5.00158-1, 1374-1390.e3, ISBN 9780323400305.

[4] Christopher I. Shaffrey, Gregory C. Wiggins, Mark F. Abel, Chapter 65 - pediatric spinal deformities, in: Edward C. Benzel (Ed.), Spine Surgery, third ed., Churchill Livingstone, 2005, pp. 824–875, https://doi.org/10.1016/B978-0-443-06616-0.50070-5. ISBN 9780443066160.

[5] L.C. Garfunkel, Jeffrey M. Kaczorowski, L.C. Garfunkel, Scoliosis, in: Pediatric clinical advisor (Second Edition) Instant Diagnosis and Treatment, 2007, pp. 510–511, https://doi.org/10.1016/B978-032303506-4.10292-5.

[6] S. Naoum, A.V. Vasiliadis, C. Koutserimpas, N. Mylonakis, M. Kotsapas, K. Katakalos, Finite element method for the evaluation of the human spine: a literature overview, J. Funct. Biomater. 12 (2021) 43, https://doi.org/10.3390/jfb12030043.

[7] P.E. Eltes, M. Bartos, B. Hajnal, A.J. Pokorni, L. Kiss, D. Lacroix, P.P. Varga, A. Lazary, Front Surg 7 (2021) 583386, https://doi.org/10.3389/fsurg.2020.583386.

[8] F. Mo, M.E. Cunningham, Pediatric scoliosis, Curr. Rev. Musculoskelet. Med. 4 (4) (2011) 175–182, https://doi.org/10.1007/s12178-011-9100-0.

[9] W. Wei, T. Zhang, Z. Huang, et al., Finite element analysis in brace treatment on adolescent idiopathic scoliosis, Med. Biol. Eng. Comput. 60 (2022) 907–920, https://doi.org/10.1007/s11517-022-02524-0.

[10] Qiaolin Zhang, TeoEe Chon, Yan Zhang, Julien S. Baker, Yaodong Gu, Finite element analysis of the lumbar spine in adolescent idiopathic scoliosis subjected to different loads, Comput. Biol. Med. 136 (2021) 104745, https://doi.org/10.1016/j.compbiomed.2021.104745. ISSN 0010-4825.

[11] I. Yamamoto, M.M. Panjabi, T. Crisco, T. Oxland, Three-dimensional movements of the whole lumbar spine and lumbosacral joint, Spine 14 (11) (1989) 1256–1260.

[12] F.H. Cheng, S.L. Shih, W.K. Chou, C.L. Liu, W.H. Sung, C.S. Chen, Finite element analysis of the scoliotic spine under different loading conditions, Bio Med. Mater. Eng. 20 (5) (2010) 251–259, https://doi.org/10.3233/BME-2010-0639.

[13] T. Guan, Y. Zhang, A. Anwar, Y. Zhang, L. Wang, Determination of three-dimensional corrective force in adolescent idiopathic scoliosis and biomechanical finite element analysis, Front. Bioeng. Biotechnol. 8 (2020) 963, https://doi.org/10.3389/fbioe.2020.00963. PMID: 32903545; PMCID: PMC7438412.

[14] Alba Gonzalez Alvarez, Karl D. Dearn, Bernard M. Lawless, Carolina E. Lavecchia, Francesco Vommaro, Konstantinos Martikos, Tiziana Greggi, E. Duncan, T. Shepherd, Design and mechanical evaluation of a novel dynamic growing rod to improve the surgical treatment of Early Onset Scoliosis, Mater. Des. 155 (2018) 334–345, https://doi.org/10.1016/j.matdes.2018.06.008. ISSN 0264-1275.

[15] P.J. Cahill, W. Wang, J. Asghar, et al., The use of a transition rod may prevent proximal junctional kyphosis in the thoracic spine after scoliosis surgery: a finite element analysis, Spine 37 (12) (2012) E687–E695, https://doi.org/10.1097/BRS.0b013e318246d4f2.

[16] N. Shimamoto, Y. Kotani, Y. Shono, et al., Biomechanical evaluation of anterior spinal instrumentation systems for scoliosis: in vitro fatigue simulation, Spine 26 (24) (2001) 2701–2708, https://doi.org/10.1097/00007632-200112150-00013.

[17] Y. Wang, G. Zheng, X. Zhang, Y. Zhang, S. Xiao, Z. Wang, Temporary use of shape memory spinal rod in the treatment of scoliosis, Eur. Spine J. 20 (1) (2011) 118–122, https://doi.org/10.1007/s00586-010-1514-7. Epub 2010 Jul 14. PMID: 20628769; PMCID: PMC3036020.

[18] J.M. Sánchez Márquez, F.J. Sánchez Pérez-Grueso, N. Fernández-Baíllo, E. Gil Garay, Gradual scoliosis correction over time with shape-memory metal: a preliminary report of an experimental study, Scoliosis 7 (1) (2012) 20, https://doi.org/10.1186/1748-7161-7-20. PMID: 23126381; PMCID: PMC3517762.

[19] D.J. Wever, J.A. Elstrodt, A.G. Veldhuizen, J.R. v Horn, Scoliosis correction with shape-memory metal: results of an experimental study, Eur. Spine J. 11 (2) (2002) 100–106, https://doi.org/10.1007/s005860100347. Epub 2001 Nov 14. PMID: 11956914; PMCID: PMC3610510.

[20] I. Villemure, C.E. Aubin, J. Dansereau, H. Labelle, Biomechanical simulations of the spine deformation process in adolescent idiopathic scoliosis from different pathogenesis hypotheses, Eur. Spine J. 13 (1) (2004) 83–90, https://doi.org/10.1007/s00586-003-0565-4.

[21] A. Rohlmann, A. Mann, T. Zander, G. Bergmann, Effect of an artificial disc on lumbar spine biomechanics: a probabilistic finite element study, Eur. Spine J. 18 (1) (2009) 89–97, https://doi.org/10.1007/s00586-008-0836-1. Epub 2008 Nov 29. PMID: 19043744; PMCID: PMC2615124.

[22] C. Öhman-Mägi, O. Holub, D. Wu, R.M. Hall, C. Persson, Density and mechanical properties of vertebral trabecular bone-a review, JOR Spine 4 (4) (2021) e1176, https://doi.org/10.1002/jsp2.1176. PMID: 35005442; PMCID: PMC8717096.

[23] D. Gehweiler, M. Schultz, M. Schulze, O. Riesenbeck, D. Wähnert, M.J. Raschke, Material properties of human vertebral trabecular bone under compression can be predicted based on quantitative computed tomography, BMC Muscoskel. Disord. 22 (1) (2021) 709, https://doi.org/10.1186/s12891-021-04571-4. Published 2021 Aug 18.

[24] R. Alkalay, The material and mechanical properties of the healthy and degenerated intervertebral disc, in: R. Barbucci (Ed.), Integrated Biomaterials Science, Springer, Boston, MA, 2002, https://doi.org/10.1007/0-306-47583-9_13.

[25] M.F. Ivicsics, N.E. Bishop, K. Püschel, M.M. Morlock, G. Huber, Increase in facet joint loading after nucleotomy in the human lumbar spine, J. Biomech. 47 (7) (2014) 1712–1717, https://doi.org/10.1016/j.jbiomech.2014.02.021.

[26] Nitinol technical properties, Johnson Matthey: https://matthey.com/products-and-markets/other-markets/medical-components/resource-library/nitinol-technical-properties [Accessed on: 10 August. 2023].

[27] A. Warburton, S.J. Girdler, C.M. Mikhail, A. Ahn, S.K. Cho, Biomaterials in spinal implants: a review, Neurospine 17 (1) (2020) 101–110, https://doi.org/10.14245/ns.1938296.148.

[28] C. Zetterberg, T. Hansson, J. Lindström, L. Irstam, G.B. Andersson, Postural and time-dependent effects on body height and scoliosis angle in adolescent idiopathic scoliosis, Acta Orthop. Scand. 54 (6) (1983) 836–840, https://doi.org/10.3109/17453678308992918.

[29] G. Torell, A. Nachemson, K. Haderspeck-Grib, A. Schultz, Standing and supine Cobb measures in girls with idiopathic scoliosis, Spine 10 (5) (1985) 425–427.

[30] M. Zhang, W. Chen, S. Wang, et al., Correlation between supine flexibility and postoperative correction in adolescent idiopathic scoliosis, BMC Muscoskel. Disord. 24 (2023) 126.

[31] S. Grycuk, P. Mrozek, Scoliosis brace finite element model and preliminary experimental testing using electronic speckle pattern interferometry, Appl. Sci. 12 (8) (2022) 3876.